NaCl-Induced Phase Separation of 1,4-Dioxane−Water Mixtures Studied by Large-Angle X-ray Scattering and Small-Angle Neutron Scattering Techniques

ARTICLE *in* THE JOURNAL OF PHYSICAL CHEMISTRY B · SEPTEMBER 2001

Impact Factor: 3.3 · DOI: 10.1021/jp011692w

7 AUTHORS, INCLUDING:

Toshiyuki Takamuku
Saga University
84 PUBLICATIONS **1,922** CITATIONS
SEE PROFILE

Masaaki Tabata
Saga University
123 PUBLICATIONS **1,835** CITATIONS
SEE PROFILE

Toshio Yamaguchi
Fukuoka University
203 PUBLICATIONS **3,783** CITATIONS
SEE PROFILE

Toshiya Otomo
High Energy Accelerator Research Organization
139 PUBLICATIONS **1,165** CITATIONS
SEE PROFILE

NaCl-Induced Phase Separation of 1,4-Dioxane−Water Mixtures Studied by Large-Angle X-ray Scattering and Small-Angle Neutron Scattering Techniques

Toshiyuki Takamuku,*,† Atsushi Yamaguchi,† Daisuke Matsuo,† Masaaki Tabata,† Toshio Yamaguchi,‡ Toshiya Otomo,§ and Tomohiro Adachi§,||

Department of Chemistry, Faculty of Science and Engineering, Saga University, Honjo-machi, Saga 840-8502, Japan, Department of Chemistry, Faculty of Science, Fukuoka University, Nanakuma, Jonan-ku, Fukuoka 814-0180, Japan, and Institute of Materials Structure Science, High Energy Accelerator Research Organization (KEK), Oho, Tsukuba 305-0801, Japan

Received: May 3, 2001; In Final Form: August 7, 2001

Salt-induced phase separation of 1,4-dioxane−water mixtures with NaCl has been investigated from the microscopic to mesoscopic scale by large-angle X-ray scattering (LAXS) and small-angle neutron scattering (SANS) methods. A phase diagram of 1,4-dioxane−water−NaCl mixtures has shown that phase separation takes place in a range of 1,4-dioxane mole fraction, $0.1 < x_{dio} \leq 0.7$. The X-ray radial distribution functions have shown that before phase separation the preferential hydration structures of Na^+ and Cl^- are enhanced with increasing NaCl concentration and that after phase separation the structures of the organic and aqueous phases are practically similar to those of 1,4-dioxane−water mixtures at the corresponding solvent compositions. The SANS data have been interpreted in terms of the Debye correlation length, L_D, as a parameter of concentration fluctuation. The L_D values were almost constant at ∼9.4 Å in the range of $0 < x_{NaCl} < \sim 0.01$, but increased quickly to ∼13 Å at $x_{NaCl} = 0.024$, which corresponds to 54% of the NaCl concentration required for phase separation. From the present findings, together with the previous results on acetonitrile−water−NaCl mixtures, a possible mechanism for NaCl-induced phase separation of 1,4-dioxane−water mixtures is discussed in terms of hydrogen bonding and dipole−dipole interaction.

Introduction

It is well-known that phase separation of organic solvent−water mixtures, such as acetonitrile−water and 1-propanol−water, occurs by addition of a suitable salt, such as NaCl.[1−3] Recently, the salt-induced phase separation of 2-propanol−water, acetonitrile−water, and 1,4-dioxane−water mixtures has been applied to extraction of highly charged species such as a metalloporphyrin which cannot be extract into conventional solvents, such as chloroform.[4,5]

Salt-induced phase separation of aqueous mixtures with water-miscible organic solvents has so far been investigated from macroscopic thermodynamics properties[6−9] and by statistical-mechanics.[10,11] Very recently, large-angle X-ray scattering (LAXS) and small-angle neutron scattering (SANS) techniques have been applied to acetonitrile−water−NaCl[12,13] and 1-propanol−water−KCl[14] systems to reveal the structures of the systems and clarify the underlying mechanism of salt-induced phase separation. In the former system, it was proposed that three factors play important roles in the phase separation: microheterogeneity, preferential hydration of Na^+ and Cl^-, and hydrogen bonds among water molecules. In particular, microheterogeneity caused by weak dipole−dipole interactions among acetonitrile and water molecules can assist phase separation in the above process.

In acetonitrile−water mixtures,[15] it was found in previous LAXS and IR measurements that acetonitrile and water molecules interact mainly by dipole−dipole interaction and microheterogeneity of individual acetonitrile and water aggregates occurs in a range of acetonitrile mole fraction (x_{AN}), $0.2 \leq x_{AN} < 0.6$. In aqueous mixtures of nonpolar 1,4-dioxane, on the other hand, previous LAXS, mass spectrometry, and NMR relaxation measurements[16] have shown that the liquid structures of the mixtures are classified into three regimes: (1) at $0.3 \leq x_{dio} < 1.0$, the neat structure observed in pure 1,4-dioxane remains, and water molecules are likely to be involved in the structure by hydrogen bonding; (2) at $0.15 \leq x_{dio} < 0.2$, both structures of water and 1,4-dioxane are disrupted to form small binary aggregates of one or two 1,4-dioxane molecules and several water molecules; and (3) at $x_{dio} \leq 0.1$ the hydrogen-bonded network of water is dominant. Thus, it is very interesting to investigate the solution structure and mechanism of salt-induced phase separation of the 1,4-dioxane−water mixtures and to compare the results with those for the acetonitrile−water−NaCl system.

In the present investigation, first, phase separation behavior of 1,4-dioxane−water−NaCl mixtures was examined at 298 K as a function of mole fractions of 1,4-dioxane (x_{dio}), water (x_W), and NaCl (x_{NaCl}), to obtain the phase diagram of the system. Then, the microscopic structures before and after phase separation of the 1,4-dioxane−water−NaCl mixtures at $x_{dio} = 0.17$, which corresponds to a 50 v/v % mixture, were determined by LAXS. Furthermore, SANS measurements were made on the 1,4-dioxane−D_2O−NaCl mixtures at $x_{dio} = 0.17$ to investigate

* Author to whom all correspondence should be addressed. Phone: +81-952-28-8554. Fax: +81-952-28-8548. E-mail: takamut@cc.saga-u.ac.jp.
† Saga University.
‡ Fukuoka University.
§ Institute of Materials Structure Science, High Energy Accelerator Research Organization (KEK).
|| Present Address: Division of Image Information, Advanced Computing Center, The Institute of Physical and Chemical Research (RIKEN), 2-1 Hirosawa, Wako 351-0198, Japan.

10.1021/jp011692w CCC: $20.00
Published on Web 09/19/2001

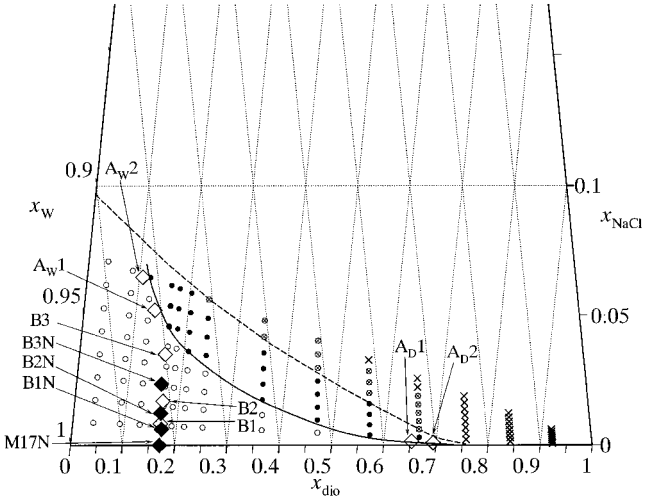

Figure 1. Phase diagram of the 1,4-dioxane−water−NaCl ternary mixtures at 298.2 ± 0.3 K as a function of mole fractions of 1,4-dioxane, x_{dio}, water, x_W, and NaCl, x_{NaCl}. The symbols of ○, ●, ×, and ⊗ represent (1) ternary mixture, (2) phase separation, (3) precipitation of NaCl, and (4) phase separation with precipitation of NaCl, respectively. The solid line represents the border between ternary mixture and phase separation, and the broken line shows the solubilities of NaCl in 1,4-dioxane−water mixtures. The compositions of sample solutions examined by LAXS (◇) and SANS (◆) are shown in the phase diagram.

aggregation in the mixtures at the mesoscopic scale. Finally, all the present findings are compared with the case for acetonitrile−water−NaCl mixtures,[12,13] and a possible mechanism of NaCl-induced phase separation of 1,4-dioxane−water mixtures is discussed.

Experimental Section

Chemical Reagents. 1,4-Dioxane (Wako Pure Chemicals, extra grade) was refluxed with metal sodium wire for 8 h, and then distilled under atmospheric pressure. NaCl (Wako Pure Chemicals, extra grade) was dried in an electric oven at 573 K for 6 h. For SANS experiments D_2O (CEA, D content = 99.9%) was used without further purification. For other experiments doubly distilled water was used.

Phase Separation Diagram. Mixing state of 1,4-dioxane−water−NaCl mixtures at 298 K was investigated in a similar way to that used in a previous study.[13] First, aqueous NaCl solutions of various NaCl concentrations were prepared by dissolving dried NaCl into distilled water. The aqueous NaCl solution thus obtained was mixed with distilled 1,4-dioxane in a graduated tube with a stopper to a required mole fraction of 1,4-dioxane. The mixed solution in the tube was vigorously shaken for 1 min and allowed to stand at 298.2 ± 0.3 K for 24 h to reach equilibrium. The state of the mixed solution was then visually examined and could be classified into four types: (1) 1,4-dioxane−water−NaCl ternary solution, (2) separation into 1,4-dioxane-rich (upper) and water-rich (lower) phases, (3) precipitation of NaCl, and (4) phase separation with precipitation of NaCl. The results were illustrated in Figure 1 as a function of mole fractions of 1,4-dioxane, x_{dio}, water, x_W, and NaCl, x_{NaCl}.

Furthermore, the chemical composition and volume of 1,4-dioxane−water−NaCl mixtures at $x_{dio} = 0.17$ were examined at 298.2 ± 0.3 K as a function of total concentration of NaCl added, $x_{NaCl,tot}$. A 5 mL volume of aqueous NaCl solution at a given NaCl concentration and 5 mL of pure 1,4-dioxane were mixed in a graduated tube with a stopper, and then the mixed solution was kept at 298.2 ± 0.3 K for 24 h. The densities of the solutions before and after phase separation were measured with a densimeter (ANTON Paar K. G., DMA 60), and the volume of the solutions was obtained from the volume-calibrated graduated tube. The concentration of Na^+ in the upper 1,4-dioxane-rich phase was determined on an atomic absorption spectrometer (Perkin-Elmer AANALYST100), whereas the concentration of Cl^- in the lower water-rich phase was determined by argentmetry using potassium chromate as an indicator. The concentration of Na^+ in the upper phase was stoichiometrically calculated from that of Cl^- in the lower phase. The concentrations of Na^+ determined by both methods were in agreement with each other within the experimental uncertainties (±0.5%). Content of water in the upper phase was determined by the Karl-Fisher titration method using an automatic titrator (Kyoto Electronics, MKL-200).

TABLE 1: Concentrations (mol dm^{-3}) and Mole Fractions, x_{dio}, x_W, and x_{NaCl}, of the Sample Solutions for LAXS and SANS Measurements

solution	[dio]	[H_2O]	[D_2O]	[NaCl]	x_{dio}	x_W	x_{NaCl}	method
N[a]	11.7				1.00			LAXS
M60[a]	10.3	6.89			0.600	0.400		LAXS
M17[a]	5.88	28.6			0.170	0.830		LAXS
M15[a]	5.44	30.7			0.150	0.850		LAXS
M10[a]	4.10	36.9			0.0999	0.900		LAXS
B1	5.37	26.2		0.261	0.169	0.823	8.20×10^{-3}	LAXS
B2	5.23	25.2		0.523	0.169	0.814	0.0169	LAXS
B3	4.99	24.3		1.06	0.164	0.801	0.0349	LAXS
A_D1	11.8	6.26		0.027	0.652	0.346	1.49×10^{-3}	LAXS
A_W1	5.01	30.0		1.92	0.136	0.812	0.0520	LAXS
A_D2	11.5	5.06		0.016	0.694	0.305	9.65×10^{-4}	LAXS
A_W2	4.20	32.8		2.56	0.106	0.829	0.0647	LAXS
M17N	5.87		28.6		0.170	0.830		SANS
B1N	5.91		28.3	0.212	0.172	0.822	6.16×10^{-3}	SANS
B2N	5.82		28.6	0.429	0.167	0.821	0.0123	SANS
B3N	5.74		28.7	0.828	0.163	0.814	0.0235	SANS

[a] Ref 16.

LAXS Measurements. LAXS measurements were made at 298 K on seven 1,4-dioxane−water−NaCl mixtures before and after phase separation on a rapid liquid X-ray diffractometer using an imaging plate (IP) as a two-dimensional detector (DIP301, MAC Science). Compositions of the sample solutions are given in Table 1, together with those of salt-free 1,4-dioxane and 1,4-dioxane−water mixtures previously investigated[16] for comparison, and also depicted in the phase diagram, Figure 1. Solutions B1, B2, and B3 are 1,4-dioxane−water−NaCl ternary mixtures before phase separation. Two pairs of solutions A_D1−A_W1 and A_D2−A_W2 correspond to the 1,4-dioxane-rich and water-rich phases separated from the ternary mixtures at $x_{dio} = 0.17$ when the total NaCl mole fractions reach $x_{NaCl} = 4.8 \times 10^{-2}$ and 6.0×10^{-2}, respectively. Densities of the sample solutions were measured with the densimeter, and the Na^+ content was determined by the atomic absorption spectrometer. Contents of water in solutions A_D1 and A_D2 were determined by the Karl-Fisher titration, while those for solutions A_W1 and A_W2 were stoichiometrically calculated from the values for solutions A_D1 and A_D2. Details of the X-ray diffractometer have been described elsewhere.[17,18] X-rays were generated at a rotary Mo anode operated at 50 kV and 200 mA, and then monochromatized by a flat graphite crystal to obtain Mo $K\alpha$ radiation ($\lambda = 0.7107$ Å). A sample solution sealed in a glass capillary of 2 mm in inner diameter was exposed to X-rays for 1 h. The observed range of the scattering angle (2θ) was from 0.2° to 109°, corresponding to the scattering vector s ($= 4\pi\lambda^{-1}\sin\theta$)

of 0.03 to 14.4 Å^{-1}. X-ray intensities for an empty capillary were also measured as background.

Two-dimensional X-ray data, $I_{obsd}(x,y)$, measured on IP were integrated into one-dimensinal data, $I_{obsd}(\theta)$, after correction for polarization as previously reported.[17,18] The observed intensities for a sample and an empty capillary were also corrected for absorption.[17,18] The contribution of a sample solution alone was obtained by subtraction of the intensities for the empty capillary from those for the sample, followed by normalization to absolute units by the conventional methods.[19−21] The structure function, $i(s)$, and the corresponding radial distribution function, $D(r)$, were calculated per stoichiometric volume V containing one 1,4-dioxane molecule in the usual manner.[15] To make a quantitative analysis of the X-ray data the theoretical structure functions calculated on a structure model were compared with the observed ones in a least-squares refinement procedure as described previously.[15] All X-ray diffraction data were analyzed by programs KURVLR[22] and NLPLSQ.[23]

SANS Measurements. Solutions of 1,4-dioxane−D_2O−NaCl mixtures were prepared by weighing 1,4-dioxane and D_2O or NaCl solutions in D_2O to $x_{dio} = 0.17$, which corresponds to a 50 v/v % mixture of 1,4-dioxane and D_2O. Densities and concentrations of NaCl for the 1,4-dioxane−D_2O−NaCl mixtures were measured as described in the previous section. All samples were prepared under nitrogen gas atmosphere in a glove box. The compositions of the sample solutions are listed in Table 1 and depicted in the phase diagram (Figure 1).

SANS intensities on mixtures M17N, B1N, B2N, and B3N were measured on the WINK spectrometer at a pulsed neutron facility (KENS) of High Energy Accelerator Research Organization (KEK), Tsukuba. A sample solution was kept in a quartz cell of 22 mm in width, 40 mm in height, and 2 mm in sample thickness, and placed in a vacuum chamber at 296.2 ± 0.5 K during measurements. The details of WINK spectrometer has been described elsewhere.[24] The wavelength (λ) range used was 1−16 Å, corresponding to the momentum transfer Q ($= 4\pi\lambda^{-1}\sin\theta$) range of 0.015−20 Å^{-1}. The neutron beam size at a sample position was 20 × 20 mm^2. SANS data were collected for 6−9 h for each solution sample. The measurements were also made on H_2O in a quartz cell of 1 mm in sample thickness, an empty cell, and background. The transmission by a sample and a cell was measured and used for absorption correction. Correction for background, absorption, cell scattering, and detector efficiencies and normalization to absolute units, were made as described in a previous paper.[14] The incoherent scattering was subtracted from the normalized intensities. All parameter values required for the above corrections were taken from the literature.[25]

Results and Discussion

Phase Separation. Figure 1 shows a phase diagram of 1,4-dioxane−water−NaCl mixtures at 298.2 ± 0.3 K. In the phase diagram the solid line shows the estimated boundary between ternary mixture and phase separation, and the broken line corresponds to the solubility of NaCl in the 1,4-dioxane−water mixtures. The scales of the mole fractions of NaCl and water are expanded for clarity because NaCl-induced phase separation takes place only in their narrow concentration ranges below the solubility of NaCl in the mixtures.

As shown in the phase diagram, phase separation of the 1,4-dioxane−water−NaCl mixtures takes place at $0.1 < x_{dio} \leq 0.7$, whereas the ternary mixtures are formed at $x_{dio} \leq 0.1$. NaCl precipitates at $x_{dio} \geq 0.25$, in particular, does at $x_{dio} > 0.7$ independent of NaCl concentration. It should be noted that for

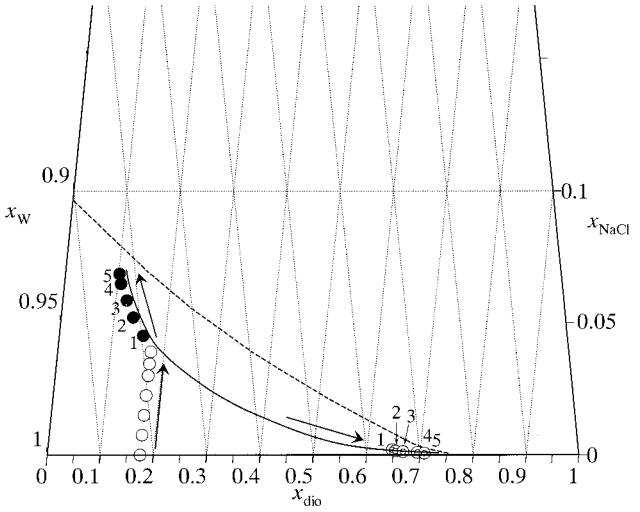

Figure 2. Compositions of 1,4-dioxane−water−NaCl mixtures at $x_{dio} = 0.17$ before phase separation (○), and 1,4-dioxane-rich (◎) and water-rich (●) phases after separation in the phase diagram of 1,4-dioxane−water−NaCl ternary mixture at 298.2 ± 0.3 K. The numbers in the phase diagram represent pairs of 1,4-dioxane-rich and water-rich phases separated from the ternary mixtures, and the arrows show the change in composition of each phase with increasing x_{NaCl}.

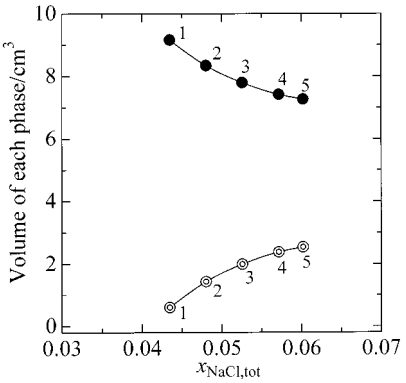

Figure 3. Volumes for 1,4-dioxane-rich (◎) and water-rich (●) phases after separation as a function of mole fraction of total NaCl, $x_{NaCl,tot}$.

acetonitrile−water−NaCl mixtures[13] phase separation occurs in a slightly wider mole fraction range of acetonitrile $0.1 < x_{AN} < 0.8$ with NaCl precipitation only in a narrower range of $x_{AN} \geq 0.57$. In both 50 v/v % mixtures ($x_{dio} = 0.17$ and $x_{AN} = 0.25$) phase separation takes place at $x_{NaCl} \geq 4.3 \times 10^{-2}$ and $x_{NaCl} \geq 9.0 \times 10^{-3}$ for the 1,4-dioxane−water mixtures and the acetonitrile−water mixtures,[13] respectively, i.e., the different microscopic interactions involved in these aqueous organic mixtures affect significantly the NaCl-induced phase separation behavior.

To obtain deeper insight into the NaCl-induced phase separation of 1,4-dioxane−water mixtures, first, changes in composition and volume of both aqueous and organic phases after phase separation were investigated at $x_{dio} = 0.17$ and are depicted in Figures 2 and 3, respectively. Figure 2 shows the compositions of the ternary mixture before phase separation and of 1,4-dioxane-rich and water-rich phases after phase separation. Figure 3 shows the volumes of 1,4-dioxane-rich and water-rich phases as a function of mole fraction of total NaCl added, $x_{NaCl,tot}$.

As shown in both figures, phase separation takes place when the NaCl mole fraction increases beyond 4.3×10^{-2}. Figure 2 reveals that the compositions of each phase after phase separation falls into the regime of the ternary solution along the

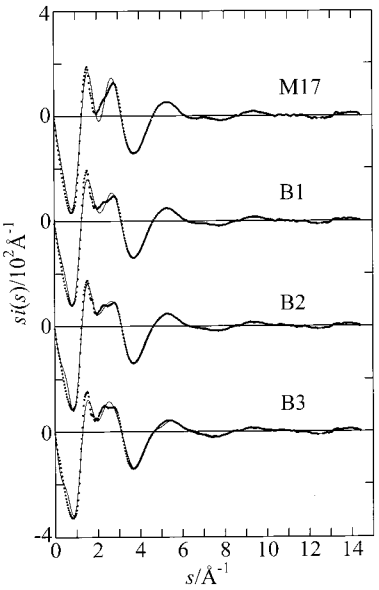

Figure 4. The *s*-weighted structure functions *i*(*s*) for solutions M17, B1, B2, and B3. The dotted and solid lines are experimental and calculated ones, respectively.

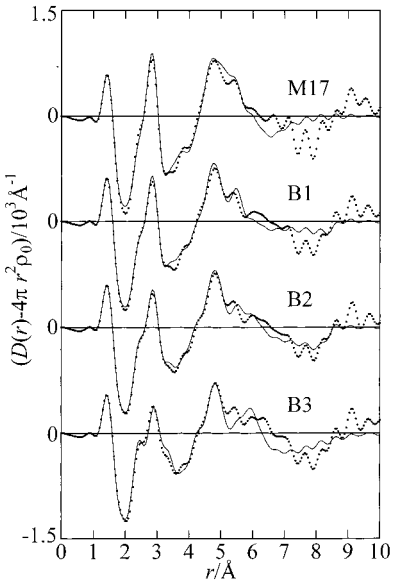

Figure 5. The radial distribution functions in the form of $D(r)\text{-}4\pi r^2\rho_0$ for solutions M17, B1, B2, and B3. The dotted and solid lines are experimental and calculated ones, respectively.

boundary between the ternary solution and phase separation. When the mole fraction of NaCl added increases up to $x_{NaCl,tot} = 6.0 \times 10^{-2}$, which is the highest NaCl concentration investigated, the 1,4-dioxane mole fraction of the water-rich phase gradually decreases, whereas that of the 1,4-dioxane-rich phase increases. On the other hand, the NaCl content in the water-rich phase proportionally increases with $x_{NaCl,tot}$ while that in the 1,4-dioxane-rich phase slightly decreases from $x_{NaCl} = 1.9 \times 10^{-3}$ to 6.5×10^{-4}, which corresponds to only ~0.2% of the added NaCl. As seen in Figure 3, with increasing NaCl concentration the volume of the 1,4-dioxane-rich phase gradually increases, but that of the water-rich phase decreases. The behaviors of the composition and volume changes for each phase are very similar to those for the acetonitrile−water−NaCl mixtures at $x_{AN} = 0.25$.[13]

These findings on the 1,4-dioxane−water−NaCl mixtures at $x_{dio} = 0.17$ imply that the preferential hydration of Na^+ and Cl^- is a driving force of the phase separation as well as phase separation of acetonitrile−water−NaCl mixtures. The Gutmann donor number (D_N) and the Mayer-Gutmann acceptor number (A_N) of 1,4-dioxane are 14.8 and 10.8, respectively, which are smaller than those (18.0 and 54.8, respectively) of water,[26] i.e., Na^+ and Cl^- would be preferentially solvated by water molecules in the 1,4-dioxane−water mixtures. In particular, solvation of Cl^- by 1,4-dioxane should be much less than by water in the mixtures due to the much smaller A_N of 1,4-dioxane. It is thus most likely that phase separation of 1,4-dioxane−water−NaCl mixtures takes place in the same manner as that for the acetonitrile−water−NaCl mixtures, i.e., water aggregates are evolved around the hydration shells of Na^+ and Cl^-, and 1,4-dioxane molecules are excluded from the water aggregates, resulting in phase separation.

Structures of 1,4-Dioxane−Water and 1,4-Dioxane−Water−NaCl Mixtures. *Before Phase Separation (Solutions M17 and B1−B3).* Figure 4 shows structure functions *i*(*s*) multiplied by *s* obtained from the LAXS measurements on the 1,4-dioxane−water−NaCl mixtures B1, B2, and B3 before phase separation. Those of a 1,4-dioxane−water mixture M17 at $x_{dio} = 0.17$ previously reported[16] are also included for comparison. The corresponding RDFs in the form of $D(r)\text{-}4\pi r^2\rho_0$ are depicted in Figure 5.

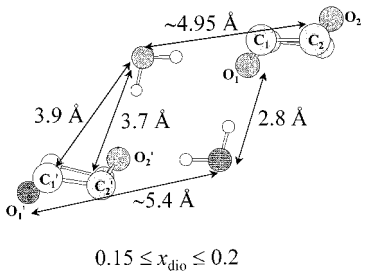

$0.15 \le x_{dio} \le 0.2$

Figure 6. Structure model for small binary aggregate of 1,4-dioxane and water molecules. Hydrogen atoms within 1,4-dioxane molecules were omitted for clarity.

Prior to interpretation of the RDFs of the 1.4-dioxane−water−NaCl mixtures, peak assignments previously made for the RDF of the corresponding NaCl-free 1,4-dioxane−water mixture M17 are briefly described here.[16] A small peak at 1.0 Å is due to the intramolecular O−H bonds within a water molecule, and a sharp peak at 1.4 Å arises from the C−C and C−O bonds within a 1,4-dioxane molecule. A shoulder at ~2.4 Å is assigned to the C···O nonbonding interaction within a 1,4-dioxane molecule. A large peak at 2.8 Å is mainly assigned to the first neighbor O···O interactions of water−water and 1,4-dioxane−water molecules. It is well-known that the O···O interactions arising from linear hydrogen bonds between water molecules appears at 2.8 Å.[27,28] The O···O interactions between 1,4-dioxane and water molecules may be attributed to hydrogen bonds between them because of electron donor and acceptor abilities of oxygen and hydrogen atoms within 1,4-dioxane and water molecules, respectively, as described above.[26] Nonbonding intramolecular C···C and O···O interactions within a 1,4-dioxane molecule also contribute to the peak. Since small aggregates of one or two 1,4-dioxane and several water molecules are mainly formed in mixtures M17 as shown in Figure 6, a large peak centered at 5 Å can be assigned to intermolecular interactions in the aggregate. The peak at ~3.9 Å corresponds to the nonbonding $C_1'\cdots O$ and $C_2'\cdots O$ interactions between 1,4-dioxane and axially closed water molecules, whereas the peak at ~4.9 Å to $C_2\cdots O$ interactions between 1,4-dioxane and equatorially closed water molecules. The large peak centered at ~5 Å matches other long-range intermolecular interactions, such as $O_1\cdots C_2'$ and $O_1\cdots$

C_1', between 1,4-dioxane molecules and partly the second neighbor O···O interaction within the tetrahedral-like structure of water.[27,28]

The RDFs for the 1,4-dioxane−water−NaCl mixtures B1, B2, and B3 do not drastically differ from that of the NaCl-free mixture M17. With increasing NaCl concentration, however, (1) a shoulder at ∼2.4 Å gradually grows, (2) a hollow at ∼3.3 Å becomes shallower and shallower, and finally, a new shoulder at ∼3.3 Å appears at the highest NaCl concentration (B3), (3) a new shoulder at ∼4.3 Å is observed for all the salt mixtures, and (4) a broad hump appears in the *r*-range of 6∼7 Å for solution B3. As discussed in the previous section, both Na^+ and Cl^- are very likely to be preferentially solvated by water molecules in the solutions. Thus, the peak at ∼2.4 Å can be assigned to the Na−O(H_2O) bonds within an octahedral $[Na(H_2O)_6]^+$.[29] The peak at ∼3.3 Å should be composed of the Cl−O(H_2O) interactions (3.14 Å) due to Cl^- hydration,[30] and the O···O interactions within $[Na(H_2O)_6]^+$ (2.4 Å$\times\sqrt{2}$ = 3.4 Å). The shoulder at ∼4.3 Å arises from the O···O interactions among hydrated water molecules within the hydration shell of Cl^-.[31] Thus, the NaCl-concentration-dependent features of RDFs for the 1,4-dioxane−water−NaCl mixtures can be reasonably interpreted in terms of the hydration of Na^+ and Cl^-, thus confirming the preferential solvation of the ions by water molecules.

To make a quantitative analysis on the structure for solutions M17, B1, B2, and B3, a comparison between the experimental structure function, *si*(*s*), and the theoretical one based on a structure model was made in *s*-space by using a least-squares refinement procedure. In the previous investigation for solution M17,[16] a peak separation procedure with Gaussian functions was applied in *r*-space to a peak at ∼2.8 Å to estimate the number of the first neighbor O···O interactions of water−water and 1,4-dioxane−water molecules, but other intermolecular interactions in the long-range ordering were not taken account. Hence, in the present study the structure of solution M17 was analyzed again by a least-squares refinement in *s*-space. First, preliminary model fits were performed in the *r*-space with taking into account the long-range interactions on the RDFs for the mixtures by using the structure parameter values of the small aggregate model (Figure 6), the tetrahedral-like structure of water, and the hydration structures of Na^+ and Cl^-. It was found that the RDFs at $r < \sim 6$ Å were explained well by the present model. Since the RDFs at $r > \sim 6$ Å contain various long-range interactions, an even electron distribution was assumed beyond ∼6 Å. Finally, a least-squares fitting procedure was carried out in the *s*-space over $0.1 \le s/\text{Å}^{-1} \le 14.4$. The finally optimized values of important parameters are listed in Table 2. As seen in Figures 4 and 5, the theoretical values of *si*(*s*) and RDFs calculated by using the values in Table 2 reproduced well the observed ones, except for the long-range interactions at $s < \sim 3$ Å^{-1} and $r \ge \sim 6$ Å not taken into account in the present analysis.

The Na−O (2.42−2.48 Å) and Cl−O (3.14−3.17 Å) distances in the first hydration shell of Na^+ and Cl^- in the mixtures are in good agreement with those (2.41 and 3.2 Å, respectively) previously determined for aqueous NaCl solutions by X-ray[29] and neutron[30] diffraction. Both distances do not change significantly within the experimental errors with increasing NaCl concentration. The hydration number (5.5 ± 0.1) of Na^+ and that (5.9 ± 0.1) of Cl^- obtained estimated for solution B3 are comparable with the values of 6.0 and 6.0, respectively, obtained in aqueous NaCl solutions.[29,30]

The number (2.54 ± 0.02) of the O···O interactions per oxygen atom within both 1,4-dioxane and water molecules for solution M17 obtained in the present analysis in the *s*-space agree within the experimental uncertainties with that (2.4 ± 0.1) estimated by the previous *r*-space analysis.[16] When the NaCl concentration increases, the number of the O···O interactions gradually decreases from (2.54 ± 0.02) in the NaCl-free solution to (2.29 ± 0.03) at $x_{NaCl} = 0.0349$. This tendency is attributed to disruption of bulk water by the increase in the hydration shells of Na^+ and Cl^-. In solution B3 the hump at 6∼7 Å is assigned probably to interactions among water molecules beyond the first hydration shells of Na^+ and Cl^-, showing enhancement of water aggregates around the ions.

On the basis of these findings, it can be concluded that the hydration structures of Na^+ and Cl^- are enhanced with increasing NaCl concentration in the 1,4-dioxane−water−NaCl mixtures before phase separation. Nevertheless, the RDFs do not show that the inherent structure of the binary mixtures is not significantly perturbed on addition of NaCl, except the hump at 6∼7 Å due to the interactions among water molecules in the second and third hydration shells of Na^+ and Cl^-. The small aggregates of 1,4-dioxane and water molecules might be partly embedded into the water aggregates around the ions due probably to hydrogen bonds between 1,4-dioxane and water molecules. Thus, the water aggregates will be less easily enhanced in the 1,4-dioxane−water mixtures with NaCl concentration than in the acetonitrile−water mixtures. This difference seems to reflect the underlying phase separation mechanism of the 1,4-dioxane−water and the acetonitrile−water mixtures.

Water-Rich Phase after Phase Separation (Solutions A_W1 and A_W2). Figure 7 shows *s*-weighted structure functions of *i*(*s*) for the water-rich phase (A_W1 and A_W2) separated from the 1,4-dioxane−water−NaCl mixtures at $x_{dio} = 0.17$. The corresponding RDFs are depicted in Figure 8. For comparison, the structure functions and the RDFs of the NaCl-free 1,4-dioxane−water mixtures at $x_{dio} = 0.1$ (M10) and 0.15 (M15), whose solvent compositions close to those of the water-rich phases, are also included in Figures 7 and 8.

As seen in Figures 5 and 8, the structures of solutions M17 and M15 are comparable with each other because of their similar compositions. In the previous study on 1,4-dioxane−water mixtures,[16] it has been found that at $0.15 \le x_{dio} \le 0.2$, small binary aggregates of one or two 1,4-dioxane and several water molecules are mainly formed in the mixtures. Thus, a peak at ∼2.8 Å in the RDF for solution M15 is assigned to the O···O distances of water−water and 1,4-dioxane−water interactions, and a large peak centered at ∼5 Å arises from intermolecular interactions within the small binary aggregates and the tetrahedral-like structure of water. The RDF for solution M10 bears resemblance to that for pure water[32] rather than that for solution M15; peaks of the first and third neighbor O···O hydrogen bonds at ∼2.8 and ∼7 Å obviously grow, and a valley at ∼5.8 Å appears. These findings suggest that the tetrahedral-like hydrogen-bonded network of water is more enhanced in solution M10 than in solution M15, and the small binary aggregates probably lessen.[16]

In the RDFs for the water-rich phases A_W1 and A_W2 shoulders are clearly observed at ∼2.4 and ∼3.3 Å; the former is assigned to the Na−O interactions within a hydration shell of Na^+,[29] whereas the latter arises from both O···O interactions among hydrated water molecules within the octahedral $[Na(H_2O)_6]^+$ (∼3.4 Å) and Cl−O interactions (3.14 Å) within a hydration shell of Cl^-.[29,30] From a comparison between Figures 5 (B1, B2, and B3) and 8 (A_W1 and A_W2) the shoulders are more

TABLE 2: Important Parameter Values of the Interactions in 1,4-Dioxane−Water and 1,4-Dioxane−Water−NaCl Mixtures before Phase Separation and Water-Rich Phase after Phase Separation by the Least-Squares Fits[a]

		solution							
interaction	parameter	M17[b]	B1	B2	B3	M15[b]	A_w1	M10[b]	A_w2
First hydration shells for Na^+ and Cl^-									
Na−O	r		2.44 (2)	2.483 (8)	2.421 (4)		2.450 (4)		2.445 (3)
	10^3b		5	5	5		4		4
	n		6.0	6.0	5.5 (1)		5.7 (1)		5.6 (1)
Cl−O	r		3.17 (2)	3.169 (8)	3.145 (4)		3.151 (4)		3.159 (4)
	10^3b		10	10	10		10		11
	n		6.0	6.0	5.9 (1)		5.7 (1)		5.6 (1)
(Na)O···O	r		3.41	3.41	3.41		3.42		3.42
	10^3b		10	10	10		10		10
	n		12.0	12.0	12.0		12.0		12.0
(Cl) O···O	r		4.30	4.30	4.30		4.30		4.30
	10^3b		10	10	10		20		20
	n		12.0	12.0	12.0		12.0		12.0
First neighbor O···O interactions of water−water and 1,4-dioxane−water									
O···O	r	2.816 (2)	2.829 (1)	2.844 (2)	2.844 (2)	2.843 (2)	2.845 (2)	2.825 (1)	2.848 (2)
	10^3b	10	10	10	10	13	12	13	12
	n	2.54 (2)	2.46 (1)	2.39 (1)	2.29 (3)	2.60 (2)	2.66 (2)	2.93 (2)	2.90 (1)
Second neighbor O···O interactions									
O···O	r	4.495 (4)	4.495 (3)	4.519 (3)	4.500 (4)	4.466 (5)	4.517 (7)	4.482 (4)	4.540 (7)
	10^3b	40	40	40	40	40	40	40	40
	n	1.28 (2)	1.51 (2)	1.41 (2)	1.35 (2)	1.22 (3)	0.87 (3)	1.26 (3)	1.11 (3)
Axially closed 1,4-dioxane and water molecules									
C_2'···O	r	3.70 (2)	3.70 (1)	3.71 (1)	3.69 (1)	3.70 (2)	3.67 (2)	3.67 (2)	3.70 (3)
	10^3b	40	40	40	40	40	40	40	40
	n	3.6 (2)	3.8 (2)	3.6 (2)	4.4 (2)	3.5 (3)	4.5 (3)	3.8 (5)	4.1 (4)
C_1'···O	r	3.90	3.90	3.90	3.90	3.90	3.90	3.90	3.90
	10^3b	40	40	40	40	40	40	40	40
	n	4.0	4.0	4.0	4.0	4.0	4.0	4.0	4.0
O_1'···O	r	4.20	4.20	4.20	4.20	4.20	4.20	4.20	4.20
	10^3b	40	40	40	40	40	40	40	40
	n	2.0	2.0	2.0	2.0	2.0	2.0	2.0	2.0
Equatorially closed 1,4-dioxane and water molecules									
C_1···O	r	3.70	3.70	3.70	3.70	3.70	3.70	3.70	3.70
	10^3b	40	40	40	40	40	40	40	40
	n	4.0	4.0	4.0	4.0	4.0	4.0	4.0	4.0
C_2···O	r	4.99 (2)	4.97 (1)	4.99 (1)	4.91 (2)	5.02 (2)	4.91 (3)	5.01 (3)	4.94 (3)
	10^3b	40	40	40	40	40	40	40	40
	n	4.5 (3)	4.4 (2)	4.8 (2)	3.5 (3)	5.1 (4)	3.0 (3)	4.0 (5)	3.9 (5)
O···O_2 (O_1')	r	5.35	5.35	5.35	5.35	5.35	5.35	5.35	5.35
	10^3b	40	40	40	40	40	40	40	40
	n	2.0	2.0	2.0	2.0	2.0	2.0	2.0	2.0

[a] The interatomic distance r(Å), the temperature factor b(Å^2), and the number of interactions n per 1,4-dioxane molecule. The values in parentheses are estimated standard deviations of the last figure. The parameters without standard deviations were not allowed to vary in the calculations. [b] Ref 16.

clearly observed in the water-rich phases than in the ternary mixtures before phase separation since the salt is more concentrated in the water-rich phases (see Table 1). The RDF for solution A_W1 beyond ∼4 Å is comparable with that for solution M15. The corresponding RDF at $r \geq \sim 4$ Å for solution A_W2 shows an intermediate feature between those for solutions M10 and M15, probably because the concentrations of 1,4-dioxane and water for solution A_W2 are between those for M10 and M15.

A quantitative analysis was made on the structure functions for the water-rich phases (A_W1 and A_W2) and also for the binary mixtures (M10 and M15), whose the number of hydrogen bonds was estimated by a peak separation procedure in the r-space in the previous study.[16] A model fitting was performed on the RDFs for the mixtures by taking into account the small aggregate model (Figure 6), the tetrahedral-like structure of water, and Na^+ and Cl^- hydration. The interactions within the r-range ≤ ∼6 Å were included, but beyond 6 Å an even electron distribution was assumed in the present analysis. A least-squares fitting procedure was performed over the s-range from 0.1 to 14.4 Å^{-1}. The optimized values of important structure parameters are summarized in Table 2. As seen in Figures 7 and 8, the theoretical $si(s)$ and RDFs calculated by using the values in Table 2 reproduced well the observed values, except the ranges at $s < \sim 3$ Å^{-1} and $r \geq \sim 6$ Å, where the interactions were not taken into account.

The parameter values determined for Na^+ and Cl^- hydration (Table 2) demonstrate that the hydration structures of Na^+ and Cl^- in the 1,4-dioxane−water−NaCl mixtures before phase separation are kept even in the water-rich phases separated from the mixtures. The intermolecular C_2···O and O···O interactions between 1,4-dioxane and water molecules in solutions A_W1 and A_W2 are not significantly different from those in solutions M10 and M15, i.e., the water-rich phase has a similar structure to that of the 1,4-dioxane−water binary mixtures at the corresponding x_{dio}.

1,4-Dioxane-Rich Phase after Phase Separation (Solutions A_D1 and A_D2). Figures 9 and 10 show the structure functions and the RDFs for the 1,4-dioxane-rich phases A_D1 and A_D2 separated from the 1,4-dioxane−water−NaCl mixtures at x_{dio}

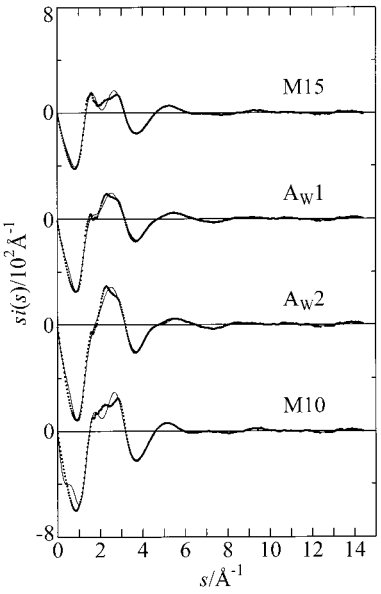

Figure 7. The *s*-weighted structure functions *i*(*s*) for water-rich phases (A_W1 and A_W2), together with those for 1,4-dioxane−water mixtures at $x_{dio} = 0.1$ and 0.15 (M10 and M15) for comparison. The dotted and solid lines are experimental and calculated ones, respectively.

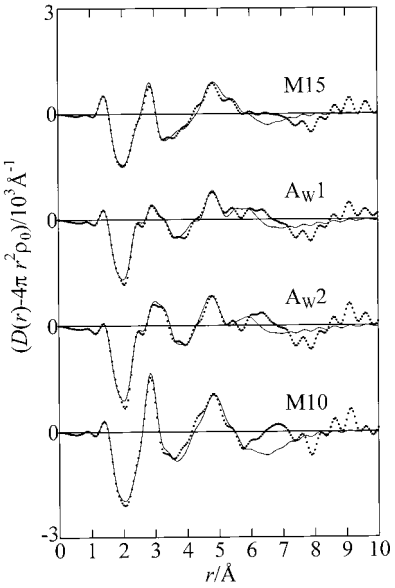

Figure 8. Radial distribution functions in the form of $D(r)$-$4\pi r^2\rho_0$ for solutions M15, A_W1, A_W2, and M10. The dotted and solid lines are experimental and calculated ones, respectively.

= 0.17. In the figures those for pure 1,4-dioxane (N) and 1,4-dioxane-water mixture at $x_{dio} = 0.6$ (M60) are also plotted for comparison.[16]

The RDF for the 1,4-dioxane−water mixture (M60) is very similar to that for pure 1,4-dioxane (N), since the neat structure of 1,4-dioxane are predominantly formed in the mixtures in the range of $x_{dio} \geq 0.3$.[16] In all the RDFs two dominant peaks and a shoulder at $r \leq 3$ Å arise mainly from intramolecular interactions within a 1,4-dioxane molecule, i.e., C−C and C−O bonds at ∼1.4 Å, C···O nonbonding interaction at ∼2.4 Å.[16] As discussed in the previous investigation,[16] a shoulder at 2.8 Å is assigned mainly to intramolecular interactions, such as C···C and O···O nonbonding interactions, within a 1,4-dioxane molecule, and partly to the first neighbor O···O interactions between 1,4-dioxane and water molecules. The very large peak centered at ∼6 Å in the RDFs is assigned to intermolecular

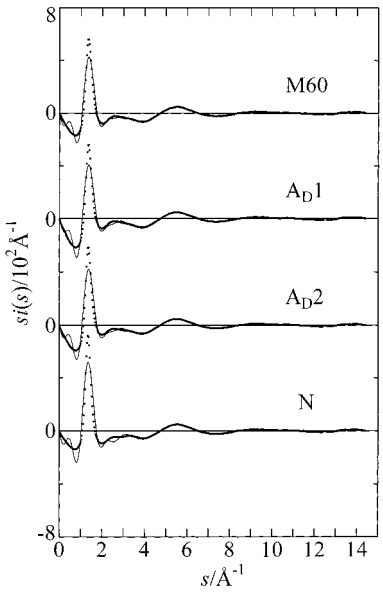

Figure 9. The *s*-weighted structure functions *i*(*s*) for 1,4-dioxane-rich phases (A_D1 and A_D2), together with those for pure 1.4-dioxane (N) and 1,4-dioxane−water mixtures at $x_{dio} = 0.6$ (M60) for comparison. The dotted and solid lines are experimental and calculated ones, respectively.

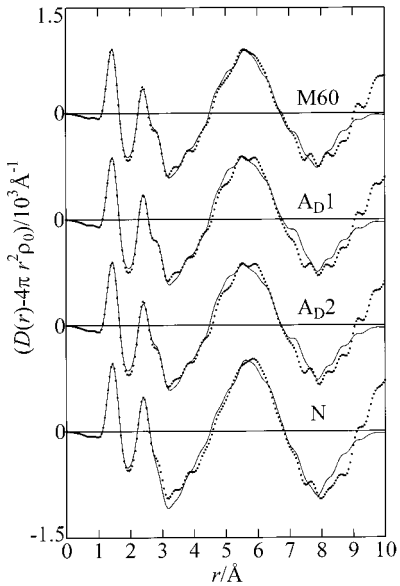

Figure 10. Radial distribution functions in the form of $D(r)$-$4\pi r^2\rho_0$ for solutions M60, A_D1, A_D2, and N. The dotted and solid lines are experimental and calculated ones, respectively.

interactions between 1,4-dioxane molecules, and/or between 1,4-dioxane and water molecules.

First, a model fitting procedure was performed on the RDFs for pure 1,4-dioxane (N)[16] in a trial-and-error manner to make a quantitative analysis on the liquid structure. However, it was difficult to build up a unique structure for pure 1,4-dioxane only from the very broad peak centered at ∼6 Å. Thus, a structural model for liquid 1,4-dioxane was built up on the basis of X-ray crystal structure of 1,4-dioxane at 279 K (phase I),[33] because the temperature (298 K) of the X-ray diffraction measurements is 13 K above the freezing point (285 K) of 1,4-dioxane. In fact, the crystal structure model explained satisfactorily the RDF for pure liquid at $r \leq$ ∼7.5 Å. The structure beyond 7.5 Å was not taken into account in the present analysis; instead, an even electron distribution was assumed for the long-range interactions.

TABLE 3: Important Parameter Values of the Interactions in Pure 1,4-Dioxane, 1,4-Dioxane−Water, and 1,4-Dioxane-Rich Phase after Phase Separation by the Least-Squares Fits[a]

		solution			
interaction	parameter	N[b]	M60[b]	A_D1	A_D2
First hydration shells for Na^+ and Cl^-					
Na−O	*r*			2.41	2.41
	10^3b			5	5
	n			6.0	6.0
Cl−O	*r*			3.14	3.14
	10^3b			10	10
	n			6.0	6.0
(Na)O···O	*r*			3.41	3.41
	10^3b			10	10
	n			12.0	12.0
(Cl) O···O	*r*			4.30	4.30
	10^3b			10	10
	n			12.0	12.0
First neighbor O···O interactions of water−water and 1,4-dioxane−water					
O···O	*r*		2.885 (8)	2.889 (6)	2.908 (8)
	10^3b		10	10	10
	n		0.89 (4)	1.05 (4)	0.94 (5)
1,4-Dioxane-1,4-dioxane interactions in a plane					
$C_1\cdots O_{2P}'$	*r*	3.50	3.50	3.50	3.50
	10^3b	40	40	40	40
	n	3.0	3.0	3.0	3.0
$O_1\cdots O_{2P}'$	*r*	4.01 (5)	3.83 (2)	3.81 (2)	3.84 (2)
	10^3b	50	50	50	50
	n	2.1 (5)	1.7 (2)	1.6 (2)	1.7 (2)
$O_1\cdots C_{1P}'$	*r*	4.70	4.70	4.70	4.70
	10^3b	50	50	50	50
	n	2.0	2.0	2.0	2.0
$O_1\cdots O_{1P}'$	*r*	5.82	5.82	5.82	5.82
	10^3b	50	50	50	50
	n	2.0	2.0	2.0	2.0
$O_1\cdots C_{4P}'$	*r*	6.00	6.00	6.00	6.00
	10^3b	50	50	50	50
	n	2.0	2.0	2.0	2.0
$C_4\cdots C_{1P}''$	*r*	4.20	4.20	4.20	4.20
	10^3b	60	60	60	60
	n	2.0	2.0	2.0	2.0
$C_4\cdots C_{2P}''$	*r*	4.37	4.37	4.37	4.37
	10^3b	60	60	60	60
	n	2.0	2.0	2.0	2.0
1,4-Dioxane−1,4-dioxane interactions between planes					
$O_1\cdots C_{4L}''$	*r*	3.90	3.90	3.90	3.90
	10^3b	50	50	50	50
	n	2.0	2.0	2.0	2.0
$O_1\cdots O_{2L}'$	*r*	4.49 (6)	4.48 (2)	4.48 (2)	4.49 (2)
	10^3b	50	50	50	50
	n	1.9 (5)	2.0 (2)	1.8 (2)	1.9 (2)
$O_1\cdots O_{1L}'$	*r*	7.10	7.10	7.10	7.10
	10^3b	50	50	50	50
	n	4.0	4.0	4.0	4.0

[a] The interatomic distance *r* (Å), the temperature factor *b* (Å^2), and the number of interactions *n* per 1,4-dioxane molecule. The values in parentheses are estimated standard deviations of the last figure. The parameters without standard deviations were not allowed to vary in the calculations. [b] Ref 16.

Finally, a least-squares refinement procedure was performed over the *s*-range from 0.1 to 14.4 Å^{-1}. The optimized important parameters are listed in Table 3. Figures 9 and 10 show good agreement between the experiments and the models except for the *s*- and *r*-ranges in which no discrete interactions were considered.

Figure 11 shows the most likely structure for liquid 1,4-dioxane with the important distances. As seen in a top view, some molecules form a plane, where the first-neighbor molecules are separated by ∼6 Å among the molecular centers. Moreover, the upper and lower molecular planes are piled by shifting ∼3 Å between the molecular centers. In the present analysis the distance and the number for the first neighbor $O_1\cdots O_{2P}'$ interactions were estimated to be (4.01 ± 0.05) Å and 2.1 ± 0.5, respectively, and those for the nearest $C_4\cdots C_{1P}''$ interactions were 4.2 Å and 2.0, respectively. The numbers estimated suggest that about four 1,4-dioxane molecules are arranged in the same plane as seen in the top view. In a side view, the distance and the number of the nearest neighbor $O_1\cdots C_{4L}''$ interactions between the upper and the lower planes are 3.9 Å and 2.0, respectively. In addition, the distances and the numbers of the second neighbor $O_1\cdots O_{2L}'$ and $O_1\cdots O_{1L}'$ interactions between the planes were estimated to be (4.49 ± 0.06) Å and 1.9 ± 0.5, and 7.10 Å and 4.0, respectively. From the present results it is likely that the planes are apart by ∼3 Å from each other with two or three planes probably piled to form an aggregate. The present LAXS results clearly show a significant structure ordering of pure liquid 1,4-dioxane despite no strong interactions between 1,4-dioxane molecules. Indeed, the long-range interactions up to ∼15 Å were clearly observed in the RDF (Figure 2 in ref 16).

Quantitative structure analyses were carried out for solutions M60, A_D1, and A_D2, as done previously. However, the parameter values for the hydration shells of Na^+ and Cl^- could not be optimized due to their very low concentrations in the 1,4-dioxane-rich phases and were thus fixed to the values obtained for the water-rich phase during the fits. The finally optimized values of important parameters are listed in Table 3. The fits between the experimental and calculated values are again good, as shown in Figures 9 and 10.

In Table 3 the structure of the 1,4-dioxane−water mixture M60 is comparable with that of pure 1,4-dioxane. In solution M60 the distance (2.885 ± 0.008) Å and the coordination number (0.89 ± 0.04) for the O···O interactions support the previous conclusion that in the range of $x_{dio} \geq 0.3$ the neat structure of pure 1,4-dioxane predominates and that water molecules may be involved into the structure by hydrogen bonding.[16] Under this situation the hydrogen bonds formed in the mixture M60 are mostly between 1,4-dioxane and water molecules.

The results in Table 3 show that the structures of the 1,4-dioxane-rich phases A_D1 and A_D2 are very similar to that for solution M60. These findings on the 1,4-dioxane-rich phase indicate that NaCl-induced phase separation of the 1,4-dioxane−water occurs when 1,4-dioxane molecules are excluded from the 1,4-dioxane−water mixtures.

The present X-ray diffraction results on the 1,4-dioxane−water−NaCl mixtures before and after phase separation, together with the macroscopic behavior such as the change in chemical composition and volume with NaCl concentration, strongly suggest that NaCl-induced phase separation of the 1,4-dioxane−water mixtures occurs in a similar way to that for acetonitrile−water−NaCl mixtures. However, it is probable that the water aggregates are less enhanced in the 1,4-dioxane−water−NaCl mixtures than the acetonitrile−water−NaCl mixtures due to the hydrogen bonds between 1,4-dioxane and water molecules.

SANS Measurements on 1,4-Dioxane−D_2O−NaCl Mixtures. Figure 12a shows SANS intensities, $I_{corr}(Q)$, for the 1,4-dioxane−D_2O−NaCl mixtures M17N, B1N, B2N, and B3N at $x_{dio} = 0.17$ and various NaCl concentrations as a function of *Q*. As seen in Figure 12 a, the SANS intensities for the mixtures at $Q \leq \sim 0.2$ Å^{-1} increase with increasing NaCl concentration, suggesting that the aggregation in the mixtures is enhanced with salt concentration. To evaluate the size of aggregates in the mixtures, the Debye correlation length, L_D,[34] was estimated as described in the previous study.[12,13] The SANS intensities, I_{corr}-

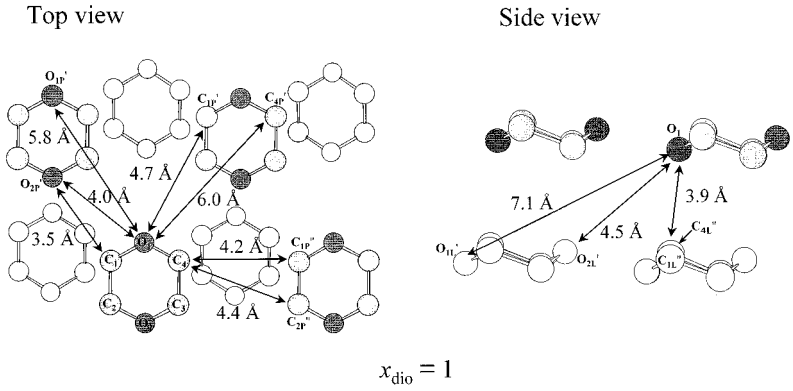

Figure 11. Structure model for pure 1,4-dioxane. Hydrogen atoms within 1,4-dioxane molecules were omitted for clarity. The shaded molecules are in the upper plane, and the nonshaded atoms in the lower one.

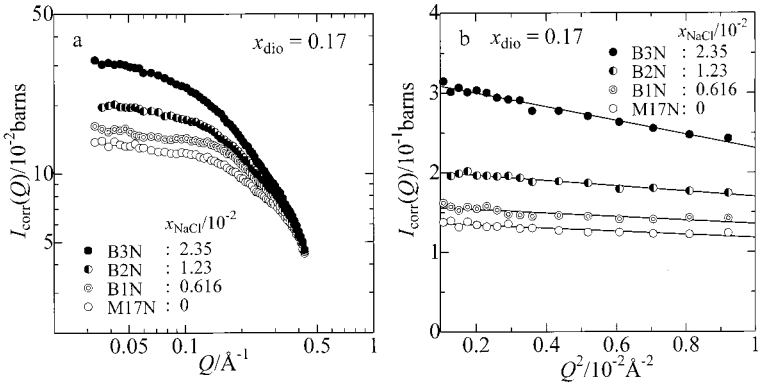

Figure 12. (a) Normalized SANS intensities for 1,4-dioxane−D_2O−NaCl mixtures at various NaCl concentrations and $x_{dio} = 0.17$ and (b) their plots of $I_{corr}(Q)$ against Q^2 values. The observed values (circles) and least-squares fitted ones (solid lines) calculated through eq 1.

TABLE 4: Debye Correlation Length L_D (Å) for 1,4-Dioxane−D_2O−NaCl Mixtures

solution	L_D
M17N	9.4(3)
B1N	9.3(4)
B2N	10.0(3)
B3N	12.8(3)

(Q), for the mixtures were plotted as a function of Q^2 in the range of $0.1 \times 10^{-2} \leq Q^2/\text{Å}^{-2} \leq 1.0 \times 10^{-2}$, and fitted with the Debye equation:

$$I_{corr}(Q) = I_0\left(1 - \frac{L_D^2}{6}Q^2\right) \quad (1)$$

where I_0 is the scattering intensity at $Q = 0$ Å^{-1}, and L_D is the Debye correlation length, by using a least-squares refinement procedure (Figure 12b). The optimized L_D values are given in Table 4 and plotted as a function of the ratio ($x_{NaCl}/x^{\circ}_{NaCl}$) of NaCl mole fraction to the critical NaCl mole fraction ($x^{\circ}_{NaCl} = 4.3 \times 10^{-2}$) required for phase separation in Figure 13.

As shown in Figure 13, the L_D value scarcely changes with increasing NaCl concentration to $x_{NaCl}/x^{\circ}_{NaCl} = 0.28$, but increases steeply to $x_{NaCl}/x^{\circ}_{NaCl} = 0.54$. The L_D value (12.8 ± 0.3) Å at $x_{NaCl}/x^{\circ}_{NaCl} = 0.54$ (B3N) is larger by a factor of ∼1.4 than that (9.4 ± 0.3) Å for the NaCl-free 1,4-dioxane−D_2O mixture (M17N). Thus, both LAXS and SANS results show that aggregation in the 1,4-dioxane−D_2O−NaCl mixtures grows with increasing NaCl concentration due to the enhanced water aggregates around the hydration shells of Na^+ and Cl^-. The behavior of the L_D value with NaCl concentration for the 1,4-dioxane−D_2O−NaCl mixtures is significantly different from that for the acetonitrile−D_2O−NaCl mixtures,[12,13] i.e., the L_D value

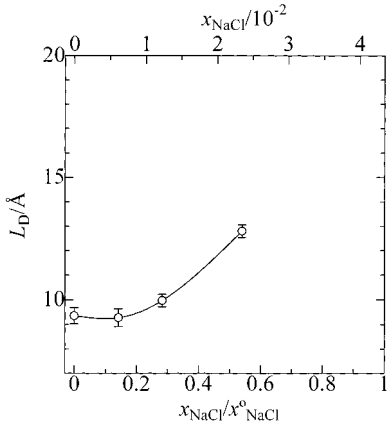

Figure 13. Debye correlation length L_D with the standard deviation of σ values as error bars for 1,4-dioxane−D_2O−NaCl mixtures as a function of NaCl mole fraction; the upper axis represents the mole fraction of NaCl, x_{NaCl}, and the lower axis gives the ratio of NaCl mole fraction to the critical NaCl mole fraction, x°_{NaCl}, required for phase separation.

for the latter rapidly increases with increasing NaCl concentration up to ∼70% of a value required for phase separation, and then has a plateau value of ∼20 Å when the NaCl concentration exceeds ∼80% of a value required for phase separation. This different behavior in L_D may be attributed to the degree of enhancement of water aggregates, i.e., the water aggregates around the hydrated Na^+ and Cl^- might be less easily formed in the former than in the latter because of hydrogen bonds between 1,4-dioxane and water. In the latter, on the contrary, water aggregates around the hydration shells of Na^+ and Cl^- could be easily formed because of weak dipole−dipole interactions among water and acetonitrile molecules.[12,13,15]

Mechanism of Phase Separation. The NaCl-induced phase separation of 1,4-dioxane−water mixtures takes place in a similar manner as for the acetonitrile−water−NaCl mixtures: (1) preferential hydration of Na^+ and Cl^- occurs in the mixtures, (2) with increasing NaCl concentration water aggregates are gradually evolved around the hydration shells of Na^+ and Cl^-, and (3) then 1,4-dioxane molecules are excluded from the water network in the process of phase separation. The hydrogen bonds between 1,4-dioxane and water molecules are probably strongly involved in processes (1) and (2), i.e., the hydrogen bonds between 1,4-dioxane and water molecules should be broken to form the preferential hydration shells of Na^+ and Cl^-, followed by formation of the water aggregates around the hydration shells of the ions as a precursor for phase separation. Since the hydrogen bonding between 1,4-dioxane and water is stronger than the dipole−dipole interaction between acetonitrile and water, the water aggregates around the hydration shells of Na^+ and Cl^- will be less easily formed for the 1,4-dioxane−water−NaCl mixtures than for the acetonitrile−water−NaCl mixtures. These differences in the microscopic structures were also reflected on the mesoscopic structures in terms of the correlation length, L_D, obtained from the SANS experiments, i.e., the L_D values starts to rise after a threshold value of NaCl concentration, ~30% of the concentration of phase separation, for the 1,4-dioxane−D_2O−NaCl mixture, in contrast with a smooth increase in L_D for the acetonitrile−D_2O−NaCl mixture.

On the basis of the above discussion, the phase diagram for the 1,4-dioxane−water−NaCl mixtures is explained as follows. In the 1,4-dioxane concentration range of $x_{dio} > 0.7$, either Na^+ and Cl^- cannot be easily hydrated by water molecules because most of water molecules are involved into the neat structure of 1,4-dioxane by hydrogen bonding, leading to precipitation of NaCl independent of NaCl mole fraction. On the other hand, for the acetonitrile−water−NaCl mixtures, where acetonitrile and water molecules interact mainly by the weak dipole−dipole interaction, NaCl precipitates only at $x_{AN} \geq 0.9$, independent of NaCl concentration. In the range of $0.1 < x_{dio} \leq 0.7$, preferential hydration shells of Na^+ and Cl^- are gradually formed because of sufficient free water molecules available, resulting in phase separation depending on NaCl mole fraction. However, the phase diagrams show that phase separation accompanied by precipitation of excess NaCl occurs in a wider range for the 1,4-dioxane−water−NaCl mixtures ($x_{dio} \geq 0.25$) than for the acetonitrile−water−NaCl mixtures (only at $0.57 \leq x_{AN} \leq 0.7$). This is also ascribed to the hydrogen bonds between 1,4-dioxane and water molecules. Furthermore, the hydrogen bonds between 1,4-dioxane and water molecules require higher NaCl concentration to initiate phase separation in the 1,4-dioxane−water−NaCl mixtures at $x_{dio} = 0.17$ ($x^\circ_{NaCl} = 4.3 \times 10^{-2}$), compared with that of the acetonitrile−water−NaCl mixtures at $x_{AN} = 0.25$ ($x^\circ_{NaCl} = 9.0 \times 10^{-3}$). In the concentration range of $x_{dio} < 0.1$, the hydrogen-bonded network of water is predominantly formed, and 1,4-dioxane molecules are probably embedded into the water network;[16] thus, 1,4-dioxane molecules, Na^+, and Cl^- are completely hydrated with water molecules, leading to the 1,4-dioxane−water−NaCl ternary mixtures.

The higher the NaCl concentration the more the phase separation of the 1,4-dioxane−water−NaCl mixtures progresses, because hydrogen bonds between 1,4-dioxane and water molecules are gradually disrupted by the strong electrostatic field of the ions with increasing NaCl concentration; thus, the 1,4-dioxane mole fraction and volume of the 1,4-dioxane-rich phase increase with added NaCl concentration.

Acknowledgment. The present work was supported partly by Grants-in-Aid (No.09740444 and No.12640500) (T.T.) and Grant-in-Aid (No.11440217) (M.T.) from the Ministry of Education, Culture, Sports, Science, and Technology, Japan.

Supporting Information Available: All optimized parameter values of the interactions in mixtures described in Tables 2 and 3 by the least squares fits. This material is available free of charge via the Internet at http://pubs.aacs.org.

References and Notes

(1) Leggett, D. C.; Jenkins, T. F.; Miyares, P. H. *Anal. Chem.* **1990**, *62*, 1355.
(2) Hawlicka, E. *Z. Naturforsch.* **1988**, *43a*, 769.
(3) Schneider, G. M. *Ber. Bunsen-Ges. Phys. Chem.* **1972**, *76*, 325.
(4) Tabata, M.; Kumamoto, M.; Nishimoto, J. *Anal. Sci.* **1994**, *10*, 383.
(5) Tabata, M.; Kumamoto, M.; Nishimoto, J. *Anal. Chem.* **1996**, *68*, 758.
(6) McDevit, W. F.; Long, F. A. *Chem. Rev.* **1952**, *51*, 119.
(7) Fromon, M.; Treiner, C. *J. Chem. Soc., Faraday Trans. 1* **1979**, *75*, 1837.
(8) Aveyard, R.; Heselden, R. *J. Chem. Soc., Faraday Trans. 1* **1975**, *71*, 312.
(9) Conway, B. E. *Pure Appl. Chem.* **1985**, *57*, 263.
(10) Haugen, G. R.; Friedman, H. L. *J. Phys. Chem.* **1963**, *67*, 1757.
(11) Krishnan, C. V.; Friedman, H. L. *J. Solution Chem.* **1974**, *3*, 727.
(12) Takamuku, T.; Matsuo, D.; Yamaguchi, A.; Tabata, M.; Yoshida, K.; Yamaguchi, T.; Nagao, M.; Otomo, T.; Adachi, T. *Chem. Lett.* **2000**, 878.
(13) Takamuku, T.; Yamaguchi, A.; Matsuo, D.; Tabata, M.; Kumamoto, M.; Nishimoto, J.; Yoshida, K.; Yamaguchi, T.; Nagao, M.; Otomo, T.; Adachi, T. *J. Phys. Chem. B* **2001**, *105*, 6236.
(14) Yoshida, K.; Misawa, M.; Maruyama, K.; Imai, M.; Furusaka, M. *J. Chem. Phys.* **2000**, *113*, 2343.
(15) Takamuku, T.; Tabata, M.; Yamaguchi, A.; Nishimoto, J.; Kumamoto, M.; Wakita, H.; Yamaguchi, T. *J. Phys. Chem. B* **1998**, *102*, 8880.
(16) Takamuku, T.; Yamaguchi, A.; Tabata, M.; Nishi, N.; Yoshida, K.; Wakita, H.; Yamaguchi, T. *J. Mol. Liquids* **1999**, *83*, 163.
(17) Yamanaka, K.; Yamaguchi, T.; Wakita, H. *J. Chem. Phys.* **1994**, *101*, 9830.
(18) Ihara, M.; Yamaguchi, T.; Wakita, H.; Matsumoto, T. *Adv. X-Ray Anal. Jpn.* **1994**, *25*, 49; Yamaguchi, T.; Wakita, H.; Yamanaka, K. *Fukuoka University Sci. Report*, **1999**, *29*, 127.
(19) Furukawa, K. *Rep. Prog. Phys.* **1962**, *25*, 395.
(20) Krogh-Moe, J. *Acta Crystallogr.* **1956**, *2*, 951.
(21) Norman, N. *Acta Crystallogr.* **1957**, *10*, 370.
(22) Johanson, G.; Sandström, M. *Chem. Scr.* **1973**, *4*, 195.
(23) Yamaguchi, T. *Doctoral Thesis*, Tokyo Institute of Technology, 1978.
(24) Furusaka, M.; Suzuya, K.; Watanabe, N.; Osawa, M.; Fujikawa, I.; Satoh, S. *KENS Report-IX* **1992**, 25.
(25) Sears, V. F. *Thermal-Neutron Scattering Lengths and Cross Sections for Condensed-Matter Research*; Chalk River Lab: Ontario, 1984.
(26) Gutmann, V. *The Donor−Acceptor Approach to Molecular Interactions*; Plenum Press: New York, 1978.
(27) Narten, A. H.; Levy, H. A. *J. Chem. Phys.* **1971**, *55*, 2263.
(28) Narten, A. H. *J. Chem. Phys.* **1972**, *56*, 5681.
(29) Caminiti, R.; Licheri, G.; Piccaluga, G.; Pinna, G. *Rend. Sem. Fac. Sci. University Cagliari* **1977**, *47*, 1.
(30) Soper, A. K.; Neilson, G. W.; Enderby, J. E.; Howe, R. A. *J. Phys. C* **1977**, *10*, 1793.
(31) Takamuku, T.; Yamagami, M.; Wakita, H.; Yamaguchi, T. *Z. Naturforsch.* **1997**, *52a*, 521.
(32) Takamuku, T.; Yamaguchi, T.; Asato, M.; Matsumoto, M.; Nishi, N. *Z. Naturforsch.* **2000**, *55a*, 513.
(33) Buschmann, J.; Müller, E.; Luger, P. *Acta Crystallogr.* **1986**, *C42*, 873.
(34) Debye, P.; MacAulay, J. *Z. Phys. Chem.* **1925**, *26*, 22.